

Supplemental Material

Reagents and antibodies

Antibody against *H3K4me1*(#5326), *H3K27ac* (# 8173), *cleaved-caspase3* (#9661), *Bax* (#2772), Phospho-*AMPKα*(Thr172) (#2535), Ubiquitin (#58395S), *DDB1*(#5428), *FLAG*-Tag (#14793), *MYC*-Tag (#2278), *HA*-Tag (#3724), Mouse *IgG1*(#5415) were from Cell Signal Technology (Boston, USA). Antibody against *Moma-2* (ab33451), α -*SMA* (ab124964), *AMPKα1* (ab32047), *MKRN1* (ab72054), *HK-2* (ab209847), Goat Anti-Rabbit IgG H&L (Alexa Fluor® 594) (ab150080), Goat Anti-Mouse IgG H&L (Alexa Fluor® 594) (ab150116), Goat Anti-Mouse IgG H&L (Alexa Fluor® 488) (ab150113), Goat Anti-Rat IgG H&L (Alexa Fluor® 488) (ab150157) were from Abcam (Cambridge, UK). Antibody against *xbp1u/s* (24168-1-AP), *GAPDH* (10494-1-AP), *CD31*(28083-1-AP), *TNF-α*(60291-1-Ig), *IL-1β*(16806-1-AP), *AMPKα2* (18167-1-AP), Phospho-*ACC1* (Ser79) (29119-1-AP), *ACC1*(21923-1-AP), *RMND5A* (17559-1-AP), *TRIM28* (15202-1-AP), *PEDF* (26045-1-AP), *CUL4A* (14851-1-AP), *CRBN* (28494-1-AP), HRP-conjugated Affinipure Goat Anti-Rabbit IgG(H+L) (SA00001-2), HRP-conjugated Affinipure Goat Anti-Mouse IgG(H+L) (SA00001-1) were from Proteintech Group, Inc. (Chicago, IL, USA). Antibody against *KSR2* (sc-100421) was from Santa Cruz Biotechnology. Antibody against *Bcl2* (A19693), *CD68* (A24386PM) was from ABclonal Biotechnology Co., Ltd. Antibody against *FBXo48* (orb183658) was from Biorbyt. Antibody against *RNF44* (HPA038981) was from AmyJet scientific (Wuhan, CHINA). TUDCA(HY-19696), Palmitic acid (HY-N0830), 2-DG(HY-13966), Cycloheximide (HY-12320), TD165(HY-130714), Lenalidomide (HY-A0003), Protein A/G Magnetic Beads (HY-K0202) were purchased from MedChemExpress (MCE, China). ox-LDL were purchased from Yiyuan

24 Biotechnologies (Guangzhou, China). MG-132(GC10383), 3-MA(GC68539),
25 Chloroquine (GC19549) were purchased from GLPBIO (Montclair, CA, USA). Puromycin
26 Solution was purchased from biosharp (Beijing, China). The atherosclerosis model diet
27 was formulated based on the Clinton-Cybulsky diet (TP28251) sourced from Trophic
28 Diets in Nantong, China, this composition includes 40% fat and 1.25% cholesterol. Total
29 Cholesterol Assay kit (Cat A111-1), Triacylglycerol Assay kit (Cat A110-1), Glucose Assay
30 kit (CAT A154-1-1) were from Nanjing Jiancheng Bioengineering Institute (Nanjing,
31 China). Fluoroshield Mounting Medium with 4',6-diamidino-2-phenylindole (DAPI,
32 ab104139) from Abcam (Cambridge, UK). Lipofectamine 2000 (11668019),
33 Lipofectamine RNAimax (13778100) were from ThermoFisher Scientific (Shanghai,
34 China). One Step Mouse Genotyping Kit (PD101-01), ChamQ Universal SYBR qPCR
35 Master Mix(Q711), HiScript III RT SuperMix for qPCR (+gDNA wiper) (R323-01) were
36 from Vazyme (Nanjing, China). Hematoxylin-Eosin/HE Staining Kit (G1120), Masson's
37 Trichrome Staining Kit(G1340), RIPA lysis buffer(R0010), Lactic acid (LA) content
38 detection kit (BC2235) were from Solarbio (Beijing, China). Oil Red O (O1516) was from
39 Sigma-Aldrich (St. Louis, MO). Trizol Reagent (Cat. No. 15596018) was from Invitrogen
40 (Grand Island, NY). Protease inhibitor cocktail (CW2200), Phosphatase Inhibitor Cocktail
41 (CW2383), SDS-PAGE Loading Buffer (CW0027) were from CWBIO (Beijing, China).
42 Immobilon ECL ultra western HRP substrate (WBULS0500) was from Millipore (Bedford,
43 MA, USA). Dual-Luciferase Reporter Assay kit (MA0518) was from MeilunBio (Dalian,
44 China). SimpleChIP® Enzymatic Chromatin IP Kit (#9005) was from Cell Signal
45 Technology (Boston, USA). EMSA probe biotin-labeling kit (GS008), Chemiluminescent

EMSA kit (GS009), BCA protein assay kit (P0012), Nuclear and Cytoplasmic Protein Extraction Kit (P0028) was from Beyotime (Shanghai, China). In Situ Cell Death Detection Kit, TMR Red (Cat. No. 12156792910) was from Roche (Indiana, IN, USA). ATP/ADP ratio chemiluminescence assay kit (E-BC-F004) was from Elabscience (Wuhan, CHINA).

Table S1

Characteristics of patients diagnosed without and with CAD. Data are presented as mean \pm SEM, n = 5 in each group. Statistical significance was determined using a two-tailed unpaired Student's t-test, with p < 0.05 considered significant. Abbreviations: BW, body weight; TC, total cholesterol; TG, triglycerides; HDL, high-density lipoprotein; LDL, low-density lipoprotein; BG, blood glucose.

	Diagnosed without CAD	Diagnosed with CAD	P value
Age (year)	55.6 \pm 5.14	52.4 \pm 4.46	0.9444
BW (Kg)	74.8 \pm 3.94	72.4 \pm 5.56	0.9683
Systolic pressure	108.8 \pm 7.91	108.4 \pm 10.58	0.9365
Diastolic pressure (mmHg)	60.2 \pm 3.7	61.2 \pm 7.4	0.8016
TC (mmol/l)	3.90 \pm 0.09	3.78 \pm 0.13	0.6667
TG (mmol/l)	1.62 \pm 0.05	1.71 \pm 0.07	0.4127
HDL (mmol/l)	1.18 \pm 0.04	1.07 \pm 0.03	0.0476

LDL (mmol/l)	2.17±0.07	2.52±0.04	0.0079
BG (mmol/l)	5.84±0.23	5.86±0.2	0.9524

Table S2
The primer sequences used for the target genes.

Genotyping the mice

Sequence	Gene Name
TGAGTGCGGACTGTTGAT	<i>KSR2</i> -F
CTTCTGGACGACTGAGGG	<i>KSR2</i> -R
TGCCTAGTCTCGGCTCTGAACTAC	APOE-F
CAACCTGGGCTACACACTAATTGAG	APOE-R

CHIP

Sequence	
AGCAAGGAGCCTAGGATTGAAA	<i>KSR2</i> (Forward)
CCGGATACCAGGATGCTCTCA	<i>KSR2</i> (Reverse)

EMSA

Sequence	
GCAGCCCTGACGCTCAGTTCC	Ref-seq (Forward)
GGAAGTGAAGCGTCAGGGCTGC	Ref-seq (Reverse)
GCAGCCCTGATGCTCAGTTCC	Alt-seq (Forward)
GGAAGTGAAGCATCAGGGCTGC	Alt-seq (Reverse)

GCTACGTTAGCCTAGTGACT	Non-specific (Forward)
AGTCACTAGGCTAACGTAGC	Non-specific (Reverse)

63

Crispr-cas9

Sequence	
AGCAAGGAGCCTAGGATTGAAA	P1-F (human)
CCGGATAACCAGGATGCTCTCA	P2-R (human)
TGCATCTTGTGCACCGATTTC	P3-F (human)
TCTTGGACACCATACGACCAG	P4-R (human)

64

RT-qPCR

Sequence	Gene Name
GAGGAGACCCAGCAAGGTTAG	<i>KSR2</i> -F (mouse)
CTGGAGTCTGGCTGGTAAGG	<i>KSR2</i> -R (mouse)
CAGGCATGAAACCCAACCTC	<i>KSR2</i> -F (human)
GGTTTCGCTTTGGCAGTTTC	<i>KSR2</i> -R (human)
GTTCCAGCGAGGGTCTACC	VCAM-1-F (mouse)
ACTCTTGGCAAACATTAGGTGT	VCAM-1-R (mouse)
TGCAAGTCTACATATCACCCAAGAA	VCAM-1-F (human)
GTAGACCCTCGCTGGAACAG	VCAM-1-R (human)
TGCCTCTGAAGCTCGGATATAC	ICAM-1-F (mouse)
TCTGTGGAACCTCCTCAGTCAC	ICAM-1-R (mouse)
CCCACAGTCACCTATGGCAA	ICAM-1-F (human)
GAGACCTCTGGCTTCGTCAG	ICAM-1-R (human)

GCAACTGTTCTGAACTCAACT	IL-1 β -F (mouse)
ATCTTTTGGGGTCCGTCAACT	IL-1 β -R (mouse)
GCCCTAAACAGATGAAGTGCT	IL-1 β -F (human)
GAACCAGCATCTTCCTCAG	IL-1 β - R (human)
CACGCTCTTCTGTCTACTG	TNF α -F (mouse)
AAGATGATCTGAGTCTGAGG	TNF α -R (mouse)
TGGCCCAGGCAGTCAGA	TNF α -F (human)
GGTTTGCTACAACATGGGCTACA	TNF α -R (human)
ATGGAATTAGAGCGCCAAGA	PFKFB3-F (mouse)
CATTTAGGTATGGCATCTCC	PFKFB3-R (mouse)
CTCGCATCAACAGCTTTGAGG	PFKFB3-F (human)
TCAGTGTTTCCTGGAGGAGTC	PFKFB3-R (human)
CAACTCCGGATGGGACAG	HK2-F (mouse)
CACACGGAAGTTGGTTCCTC	HK2-R (mouse)
GAGCCACCACTCACCTACT	HK2-F (human)
CCAGGCATTCGGCAATGTG	HK2-R (human)
TGTCTCTGGAGGAGAGCTATTTGA	<i>AMPKα1</i> -F (mouse)
GGTGAGCCACAGCTTGTCTT	<i>AMPKα1</i> -R (mouse)
GGAGCCTTGATGTGGTAGGAA	<i>AMPKα1</i> -F (human)
TCAAATAGCTCTCCTCCTGAGAC	<i>AMPKα1</i> -R (human)
CAGAAGATTCGCAGTTTAGATGTTGT	<i>AMPKα2</i> -F (mouse)
ACCTCCAGACACATATTCCATTACC	<i>AMPKα2</i> -R (mouse)

TCCTCAACACCTCAGCGTTC	<i>AMPKα2</i> -F (human)
CTTCCGGTCAAAGAGCCAGT	<i>AMPKα2</i> -R (human)
GGCTGTATTCCCCTCCATCG	β -actin- F (mouse)
CCAGTTGGTAACAATGCCATGT	β -actin- R (mouse)
CATGTACGTTGCTATCCAGGC	β -actin- F (human)
CTCCTTAATGTCACGCACGAT	β -actin- R (human)

65

66

Table S3

67

Sequences of gene-shRNA.

Gene Name	Sequence
Xbp1s-siRNA (human)	UAGAAAAUCAGCUUUUACGAGAGAA
<i>KSR2</i> - siRNA#1 (human)	CCCUCUAGUCAUCAGAAUAAGAGCA
<i>KSR2</i> - siRNA#2 (human)	GGGUUACUCAAAACAAACAAUCCAAA
<i>KSR2</i> - siRNA#3 (human)	CCTCAGGAATGTCCACATGTC
<i>CUL4A</i> -siRNA (human)	AAGAAGAUUAACACGUGCUGG
<i>CRBN</i> -siRNA (human)	AAGTGCCAGATATTTCTTCA
MKRN1- siRNA (human)	CACAGGCG AAGCTGAGTCAAG
<i>RMND5A</i> - siRNA (human)	CACCAUAUGUUCACCUACU
TRIM28- siRNA (human)	GCAUGAACCCCUUGUGCUG
PEDF- siRNA (human)	GGAAAUUCCCGAUGAGAUCUUTT
FBXo48- siRNA (human)	Santa cruz (#sc-94411)
RNF44- siRNA (human)	CGUUCAUGGUUGAUCUCCACG
<i>AMPKα1</i> - siRNA#1(human)	CAAAGUCGACCAAUGAUA

<i>AMPKα1</i> - siRNA#2 (human)	GAAGGUUGGCAAACAUGAATT
---	-----------------------

68

69 Table S4

70 **SNPs in High Linkage Disequilibrium with rs11830157 ($r^2 \geq 0.8$) in CHB, GIH, or CEU**

71 **Populations.** Abbreviations: Ref, reference allele; Alt, alternative allele; MAF, minor allele
72 frequency; CHB, HAn Chinese in Beijing, China; GIH, Gujarati Indian from Houston, Texas;
73 CEU, Utah Residents (CEPH) with Northern and Western European Ancestry

snp	Allele		LD Coefficient with rs11830157 (r^2)			Location	Distance (bp)
	Ref>Alt	MAF	CHB	GIH	CEU		
rs12814988	T>G	0.25	0.69242	1	0.603445	12:117827344	292
rs874560	T>C	0.28	0.69242	1	0.711249	12:117830660	3024
rs7136032	C>T	0.28	0.69242	1	0.711249	12:117831465	3829
rs12825364	A>G	0.28	0.69242	1	0.687151	12:117832826	5190
rs1155759	G>A	0.24	0.69242	0.978	0.628376	12:117835671	8035
rs1074482	C>T	0.26	0.662649	0.935	0.30759	12:117845711	18075
rs71099081	T ₁₁ >T ₁₀ / T ₁₂	0.003/ 0.094	0.558157	0.914	0.54046	12:117840106 -117840116	12470
rs12822146	C>T	0.16	0.662649	0.893	0.37237	12:117837586	9950

74

75 Table S5

76 **Polar interactions between *KSR2* and *AMPK α 1*.** PDBePISA was used to analyze the
77 HADDOCK-predicted binding model. Note that the *AMPK α 1* protein structure (6C9H) is
78 incomplete; therefore, the predicted *AMPK α 1* sites in this model correspond to actual sites
79 (Q13131) with an additional 9 residues.

	Residues in <i>KSR2</i>	Distance (Å)	Residues in <i>AMPKα1</i>
Hydrogen bonds			
1	CYS 348(N)	3.80	ASP 22(OD2)
2	GLN 354(N)	3.85	ASP 105(OD1)

3	ARG 366(HE)	1.69	ASP 114(OD2)
4	HIS 372(NE2)	3.63	GLN 319(O)
5	HIS 342(O)	3.09	GLY 11(N)
6	SER 343(O)	2.97	GLY 11(N)
7	SER 347(O)	2.74	ASP 22(N)
8	GLU 349(OE1)	1.84	LYS 43(HZ1)
9	PRO 374(O)	1.89	ARG 74(HH21)
10	THR 379(OG1)	2.08	GLN 83(HE21)
11	GLU 385(OE1)	3.39	SER 89(N)
Salt bridges			
1	ARG 366(NE)	2.69	ASP 114(OD2)
2	ARG 366(NH2)	3.50	ASP 114(OD2)
3	GLU 349(OE1)	2.67	LYS 43(NZ)
4	GLU 349(OE2)	3.06	LYS 43(NZ)

80

81

82

83

84

Figure S1

Coronary artery disease (CAD) associated SNP rs12822146 allelic variation correlates with *KSR2* Expression in endothelial cells. **A**, The region encompassing all common SNPs

with $r^2 \geq 0.8$ with respect to the SNP rs11830157 in CHB (Han Chinese in Beijing, China) , GIH(Gujarati Indian from Houston, Texas), CEU(Utah Residents (CEPH) with Northern and Western European Ancestry) population. The DNaseI, CTCF, *H3K4me1*, and *H3K27ac* signals surrounding this region were visualized using publicly available ENCODE datasets on the UCSC Genome Browser [Expanded Encyclopedias of DNA Elements in the Human and Mouse Genomes]. Data from aortic, thoracic aortic, and coronary artery tissues from different patients were used for analysis. Blue dashed boxes indicate regions of open chromatin, the red dashed line marks the position of SNP rs12822146. **B** and **C**, ChIP-qPCR showing no enhancer activity in the region surrounding rs12822146 in **(B)** smooth muscle cells and **(C)** macrophages. Pulldown of *H3K4me1* (mono-methyl-histone H3 lysine 4), *H3K27ac* (acetyl-histone H3 lysine 27) was performed to assess the enrichment of chromatin fragments containing rs12822146. $n = 5$, 2-tailed unpaired Mann-Whitney U test due to small sample sizes. **D** and **E**, ChIP-qPCR showing no specific binding of **(D)** MEIS1 or **(E)** GATA2 to the region surrounding rs12822146 in endothelial cells, with or without oxLDL stimulation (100 $\mu\text{g/mL}$). $n = 6$, 2-tailed unpaired Student's t-test. **F** and **G**, ChIP-qPCR showing no specific binding of XBP1s to the region surrounding rs12822146 in **(F)** smooth muscle cells and **(G)** macrophages, with or without oxLDL stimulation (100 $\mu\text{g/mL}$). $n = 5$, 2-tailed unpaired Mann-Whitney U test due to small sample size. **H**, Competitive EMSA demonstrating allele-specific competitive binding of nuclear proteins from endothelial cells to the rs12822146 locus. **I** and **J**, HUVECs were transfected with TUDCA (10 $\mu\text{mol/L}$, 24h) or DMSO for 48 h, followed by treatment with or without oxLDL (100 $\mu\text{g/mL}$) for 24 h. **(I)** RT-qPCR and **(J)** western blot showing changes in *KSR2* expression. $n = 6$. 2-tailed unpaired Student's t-test, except for the left panel in **J** employed 2-tailed unpaired Mann-Whitney U test due to non-normal distribution. ns, not significant.

A

B

C

D

E

F

G

H

Labeled-Ref	+ + + + + +
Unlabeled-Alt	- ×10 ×25 ×50 ×100 -
Non-specific probe	- - - - - ×100
Nuclear Extract	+ + + + + +

I

J

111

112

113

114

115

116

Figure S2

Localization and dynamics of *KSR2* expression within atherosclerotic plaques. A and B, Immunofluorescence staining of cryosections from intermediate and advanced coronary lesions showing *KSR2* localization in **(A)** smooth muscle cells and **(B)** macrophages. *KSR2* is shown in red, α -SMA or CD68 in green, and nuclei (DAPI) in blue. Scale bars = 100 μ m. EC, endothelial cells; N, neointima; M, media; A, adventitia. White dashed lines indicate the endothelial boundary within the plaque. **C,** Immunofluorescence staining of mouse aortic cryosections showing *KSR2* localization within atherosclerotic plaques. *KSR2* is shown in red; CD31, α -SMA, or CD68 in green; and nuclei (DAPI) in blue. Scale bars = 100 μ m. L, lumen. **D-F,** Western blot analysis of *KSR2* expression in **(D)** primary aortic endothelial cells, **(E)** aortic smooth muscle cells, and **(F)** peritoneal macrophages isolated from mice fed a high-fat diet for 0, 4, 8, and 12 weeks. n = 5, Kruskal-Wallis test with Dunn's multiple comparisons test due to small sample sizes. ns, not significant.

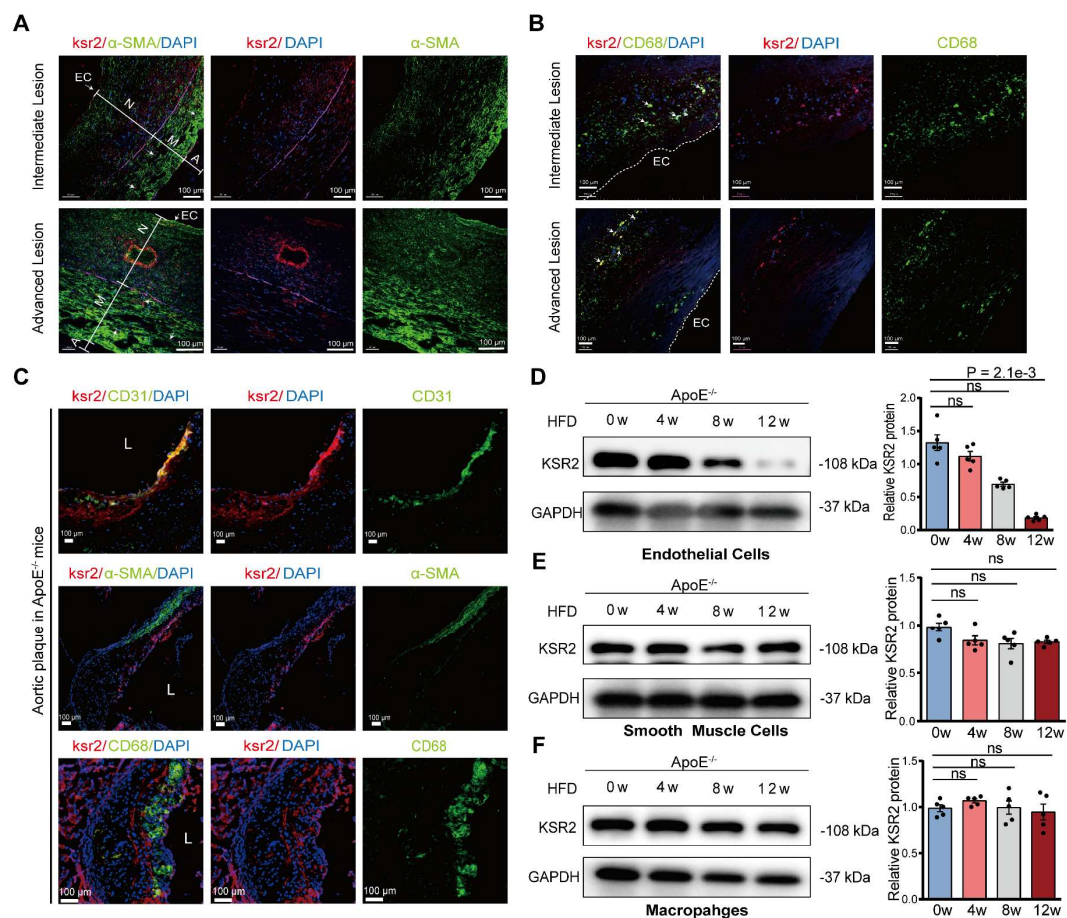
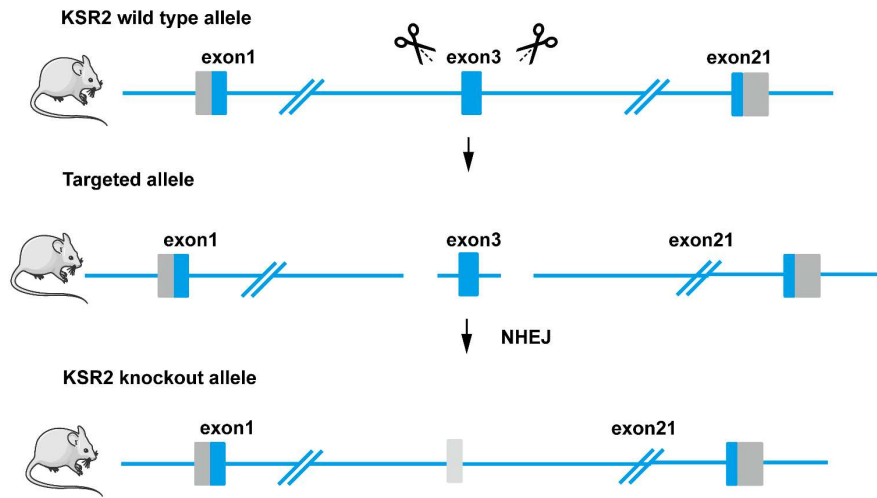


Figure S3

General Characteristics of wild-type (WT) and *KSR2*^{-/-} mice. Eight-week-old WT and *KSR2*^{-/-} mice were fed a high-fat diet (HFD) ad libitum for 12 weeks. **A**, Schematic diagram of *KSR2* knockout mice. **B and C**, Western blot (**B**) and RT-qPCR (**C**) analyses of aortic tissue were performed to verify *KSR2* knockout efficiency. n = 8, 2-tailed unpaired Mann–Whitney U test due to non-normal distribution. **D–K**, Measurements of (**D**) body weight, (**E**) serum triglycerides, (**F**) low-density lipoprotein cholesterol (LDL-C), (**G**) high-density lipoprotein cholesterol (HDL-C), (**H**) total cholesterol, (**I**) blood glucose levels, (**J**) serum insulin levels and (**K**) HOMR-IR index in WT and *KSR2*^{-/-} mice. n = 6. 2-tailed unpaired Student's t-test, except for serum triglycerides (**D**), which were analyzed using the 2-tailed unpaired Mann–Whitney U test due to non-normal distribution. HOMA-IR = fasting insulin (μIU/mL) × fasting glucose (mmol/L) / 22.5. ns, not significant.

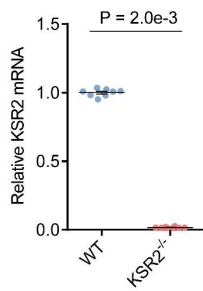
A



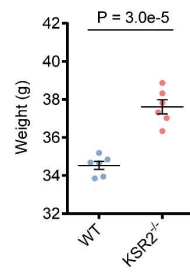
B



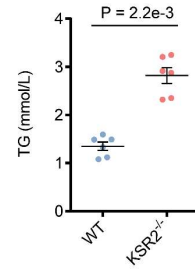
C



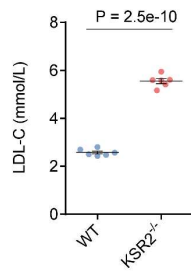
D



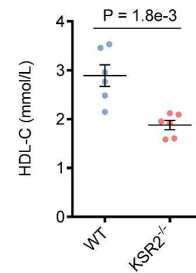
E



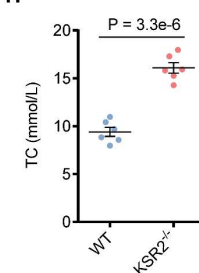
F



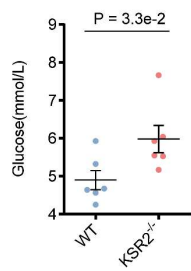
G



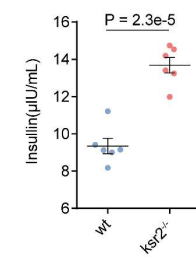
H



I



J



K

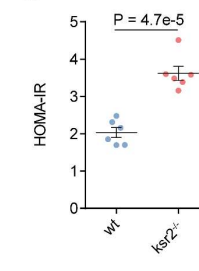


Figure S4

General characteristics of *Apoe*^{-/-} and *Apoe*^{-/-}*KSR2*^{-/-} mice. Eight-week-old *Apoe*^{-/-} and *Apoe*^{-/-}*KSR2*^{-/-} mice were pair-fed a high-fat diet (HFD) for 12 weeks. Measurements of (A) body weight, (B) serum triglycerides, (C) low-density lipoprotein cholesterol (LDL-C), (D) high-density lipoprotein cholesterol (HDL-C), (E) total cholesterol, (F) blood glucose levels, (G) serum insulin levels and (H) HOMR-IR index in *Apoe*^{-/-} and *Apoe*^{-/-}*KSR2*^{-/-} mice. n = 10. 2-tailed unpaired Student's t-test, except for serum triglycerides (B), which were analyzed using the 2-tailed unpaired Mann–Whitney U test due to non-normal distribution. HOMA-IR = fasting insulin (μIU/mL) × fasting glucose (mmol/L) / 22.5. ns, not significant.

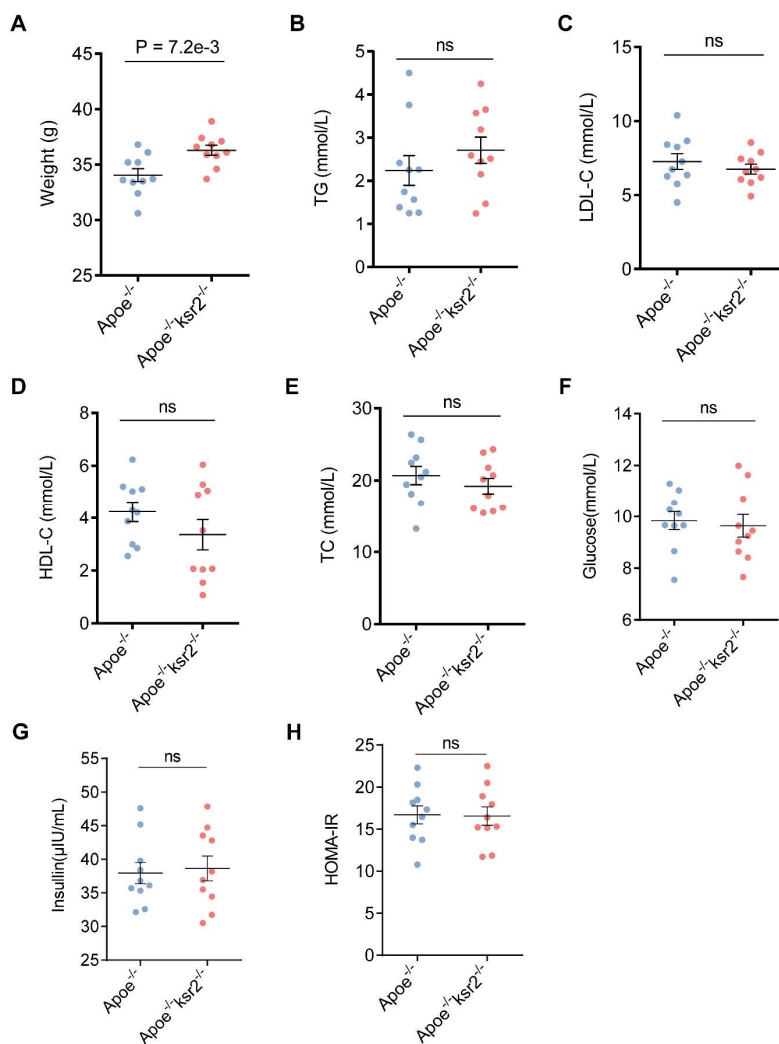


Figure S5

Metabolic profile of *Apoe*^{-/-} mice with endothelial-specific overexpression of *KSR2*. Eight-week-old *Apoe*^{-/-} mice received tail vein injections of equal doses of AAV9-ICAM2-*KSR2* (AAV9-*KSR2*) or AAV9-ICAM2-mock (AAV9-mock), followed by 12 weeks of high-fat diet feeding. **A**, Ex vivo imaging was used to detect the successful, vascular-specific distribution of AAV9-*KSR2* in *Apoe*^{-/-} mice following tail vein injection. Scale bar = 5 mm. **B**, RT-qPCR analysis of *KSR2* mRNA levels in the aortic tissue of *Apoe*^{-/-} + AAV9-mock and *Apoe*^{-/-} + AAV9-*KSR2* mice. n = 5, 2-tailed unpaired Mann-Whitney U test due to small sample sizes. **C-H**, Measurements of **(C)** body weight, **(D)** serum triglycerides, **(E)** low-density lipoprotein cholesterol (LDL-C), **(F)** high-density lipoprotein cholesterol (HDL-C), **(G)** total cholesterol, **(H)** blood glucose levels, **(I)** serum insulin levels and **(J)** HOMR-IR index in *Apoe*^{-/-} + AAV9-mock and *Apoe*^{-/-} + AAV9-*KSR2* mice. n = 8, 2-tailed unpaired Student's t-test. HOMA-IR = fasting insulin (μIU/mL) × fasting glucose (mmol/L) / 22.5. ns, not significant.

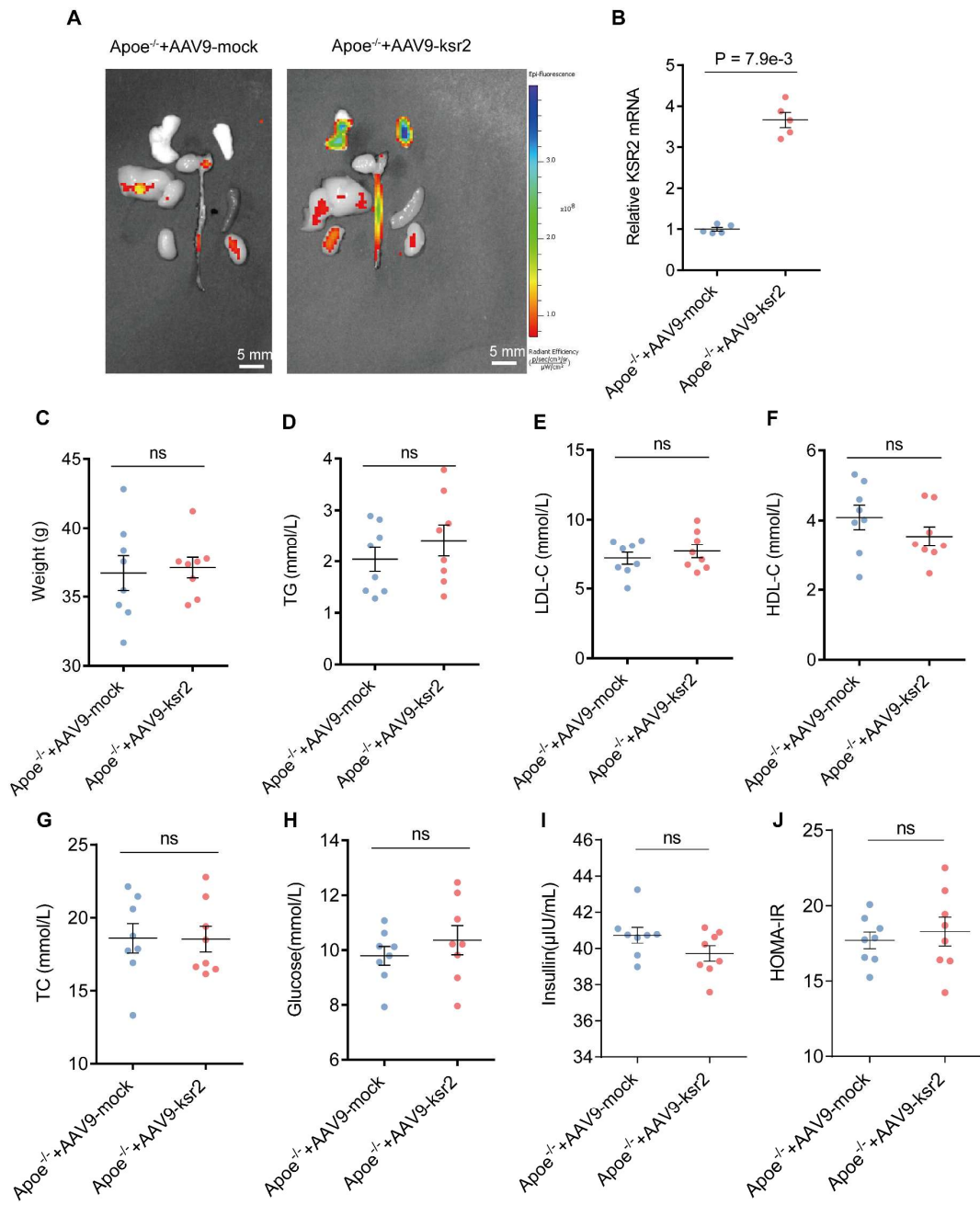


Figure S6

Effect of palmitic acid stimulation on endothelial *KSR2* expression. Western blot and RT-qPCR analyses were performed to assess *KSR2* expression in HUVECs following time-course stimulation with palmitic acid (PA, 200 μ mol/L). Relative expression levels were normalized to the 0 h control group. n = 5, Kruskal-Wallis test with Dunn's multiple comparisons test due to small sample sizes.

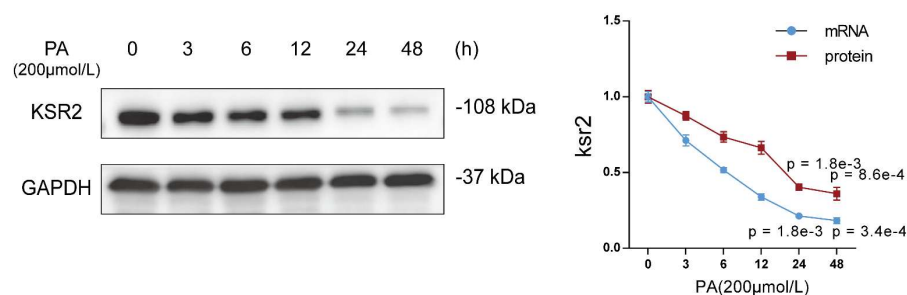


Figure S7

RNA-Seq analysis reveals the regulatory role of *KSR2* in HUVECs. A, Western blot analysis was used to detect *KSR2* expression in lentiviral stable-transfected HUVECs overexpressing *KSR2* (lenti-*KSR2*) and control (lenti-NC) cells. **B**, Volcano plots showing differentially expressed genes (DEGs) in lenti-NC and lenti-*KSR2* HUVECs. The plot highlights 535 upregulated genes (represented by red dots) and 444 downregulated genes (represented by green dots). *n* = 3. **C**, KEGG pathway analysis of DEGs identified in lenti-NC and lenti-*KSR2* HUVECs. **D**, GO enrichment analysis of DEGs identified in lenti-NC and lenti-*KSR2* HUVECs.

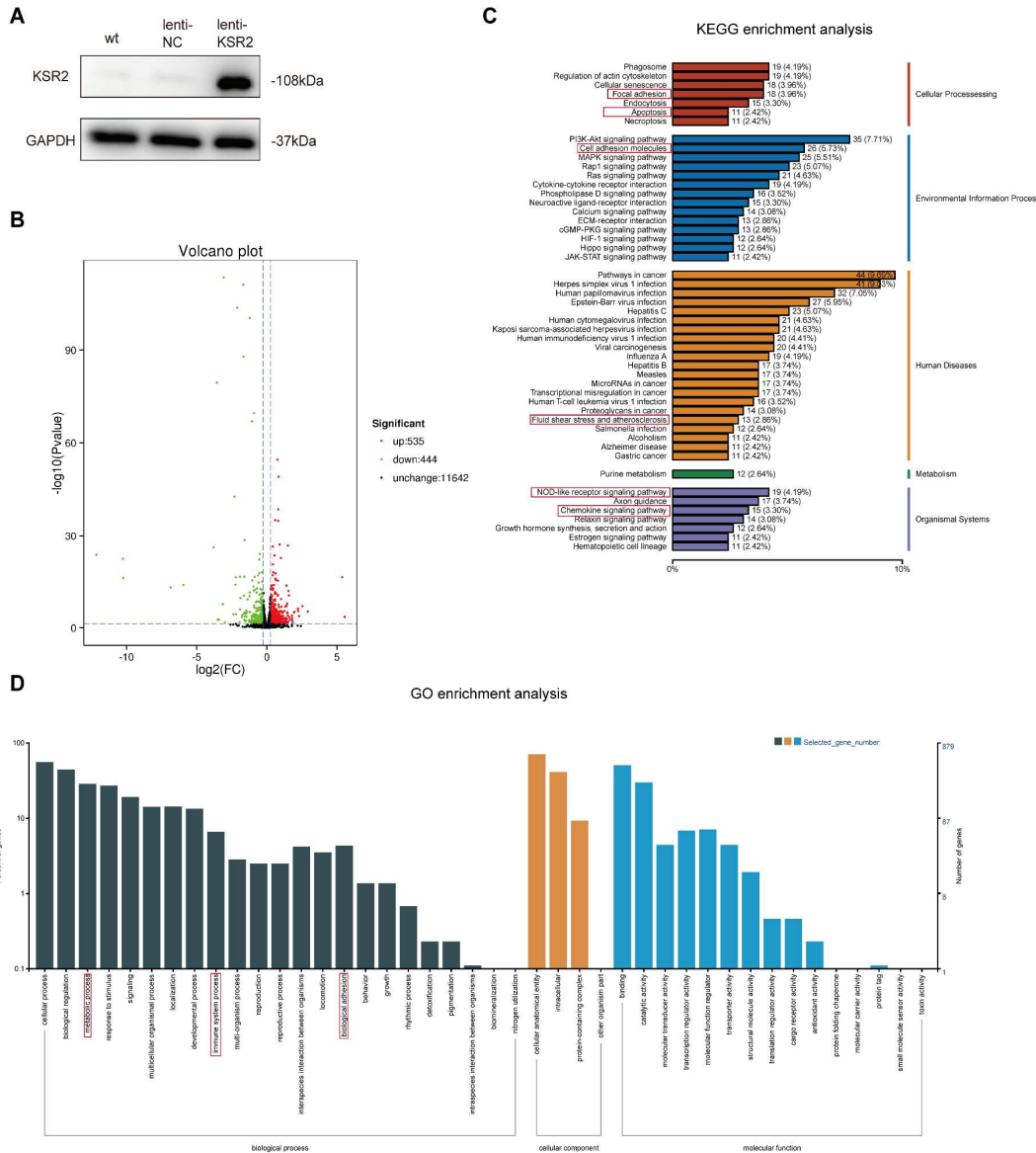


Figure S8

Validation of *KSR2* knockdown efficiency in HUVECs. RT-qPCR analysis confirmed that siRNA-mediated knockdown of *KSR2* (si-*KSR2*) significantly reduced *KSR2* mRNA levels in HUVECs. $n = 5$; Kruskal–Wallis test with Dunn’s multiple comparisons test was used due to small sample sizes. ns, not significant.

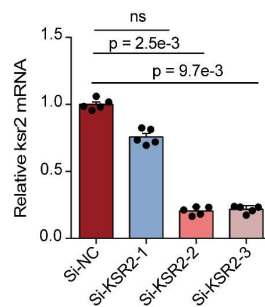


Figure S9

Endothelial *KSR2* mitigates atherosclerosis by inhibiting inflammation and apoptosis. A, Immunohistochemical staining of VCAM-1, ICAM-1, *TNF- α* , and IL-1 β in the aortic roots of *Apoe*^{-/-} + AAV9-mock and *Apoe*^{-/-} + AAV9-*KSR2* mice. Scale bar = 400 μ m. $n = 8$, 2-tailed unpaired Student’s t-test. **B,** Representative en face TUNEL staining of endothelial cells in the aorta of *Apoe*^{-/-} + AAV9-mock and *Apoe*^{-/-} + AAV9-*KSR2* mice. TUNEL-positive cells are shown in red, *CD31* in green, and nuclei (DAPI) in blue. Scale bar = 20 μ m. $n = 5$, 2-tailed unpaired Mann–Whitney U-test due to small sample sizes. **C,** Western blot analysis of cleaved caspase-3, Bcl-2, and *Bax* protein levels in aortic tissues from *Apoe*^{-/-} + AAV9-mock and *Apoe*^{-/-} + AAV9-*KSR2* mice. $n = 6$, Statistical analysis of *Bax*/Bcl-2 results was performed using a 2-tailed unpaired Mann–Whitney U test due to non-normally distributed data, cleaved caspase-3 results were analyzed using a 2-tailed unpaired Student’s t-test. **D, E, F and G,** HUVECs were transfected with Lenti-NC or Lenti-*KSR2* for 48 h, followed by treatment with oxLDL (100 μ g/mL) for 24 h. **(D)** RT-qPCR was used to measure the mRNA levels of VCAM-1, ICAM-1, *TNF- α* , and IL-1 β . $n = 6$, 2-tailed Mann–Whitney U tests (multiple t-test framework, one per gene) with Bonferroni adjustment to control the family-wise error rate. **(E)** THP-1 adhesion assay assessing the adhesive capacity of HUVECs following *KSR2* overexpressed. Results are presented as the percentage of endothelial cells with adherent THP-1 cells. Scale bar = 400 μ m. $n = 6$, 2-tailed unpaired Student’s t-test. **(F)** TUNEL staining analysis of apoptosis in HUVECs following *KSR2* overexpressed. Results are presented as the percentage of TUNEL-positive cells. Scale bar = 200 μ m. $n = 6$, 2-tailed unpaired Student’s t-test. **(G)** WB analysis was used to assess the protein levels of cleaved caspase-3, Bcl-2, and *Bax*. $n = 6$, 2-tailed unpaired Student’s t-test.

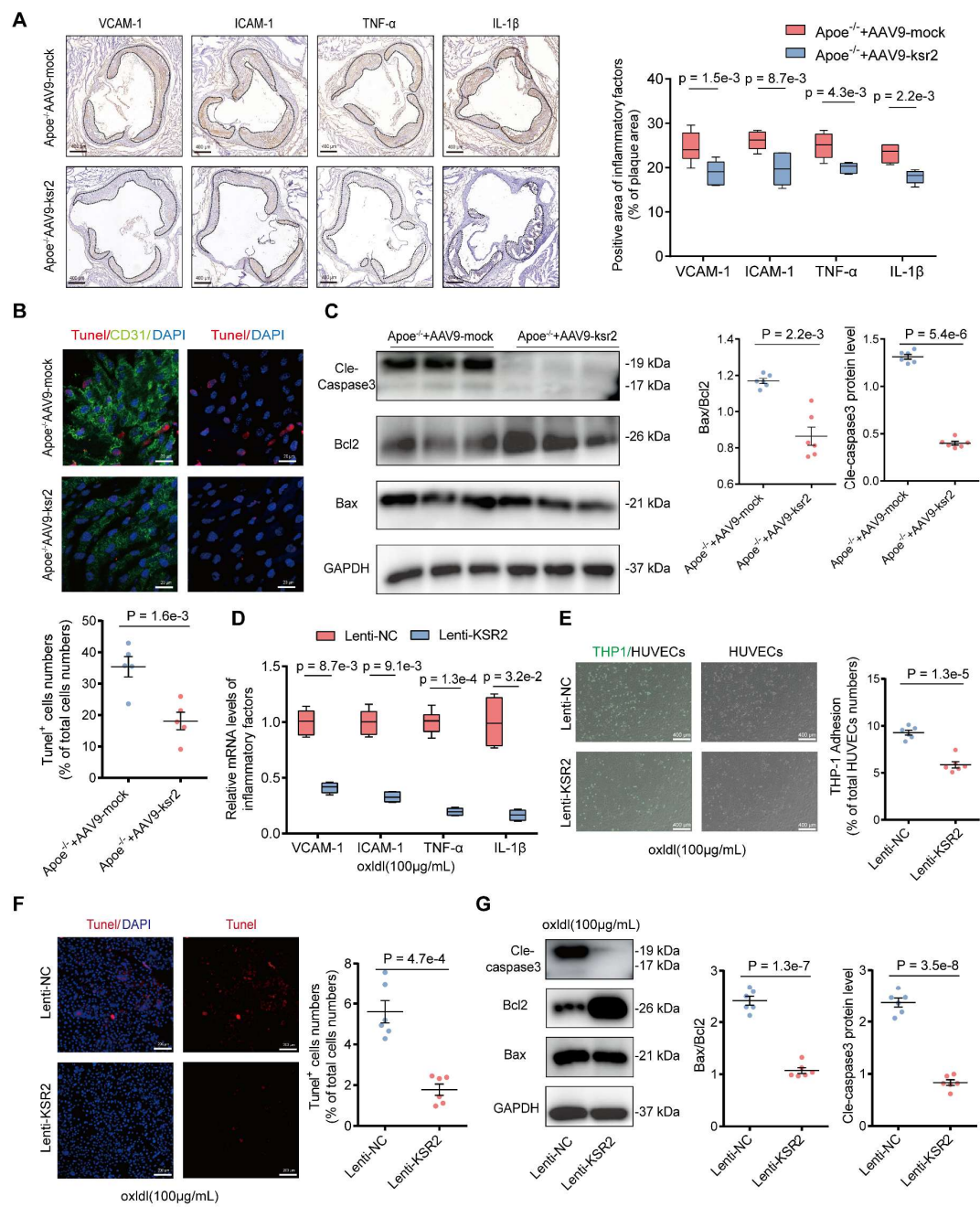


Figure S10

KSR2 overexpression in HUVECs maintains glycolytic balance. A-C, lenti-KSR2 and lenti-NC HUVECs were treated with oxLDL (100 µg/mL) or control for 24 h. **(A)** RT-qPCR analysis of mRNA levels of *HK-2* (left) and *PFKFB-3* (right) in the cells. n = 6, ordinary one-way ANOVA. **(B)** The extracellular acidification rate (ECAR) profile was used to assess the glycolytic function of HUVECs. Vertical lines indicate the addition of glucose (10 mM), oligomycin (1 µM), and 2-DG (50 mM). n = 10, Kruskal–Wallis test with Dunn’s multiple comparisons test due to non-normally distributed data. **(C)** The cellular ATP/ADP ratio was determined to evaluate energy metabolic shifts in HUVECs. n = 6, ordinary one-way ANOVA. **D**, RT-qPCR analysis of *PFKFB3* and *HK2* mRNA levels in the aortic tissues of *Apoe*^{-/-} + AAV9-mock and *Apoe*^{-/-} + AAV9-KSR2 mice. n = 6, 2-tailed Mann–Whitney U tests (multiple t-test framework, one per gene) with Bonferroni adjustment to control the family-wise error rate. **E**, Representative en face immunofluorescence staining of *PFKFB3* and *HK-2* in endothelial cells of the aorta from *Apoe*^{-/-} + AAV9-mock and *Apoe*^{-/-} + AAV9-KSR2 mice. *PFKFB3* or *HK-2* is shown in red, *CD31* in green, and DAPI in blue. Scale bar = 40 µm. n = 6, 2-tailed unpaired Student’s t-test. ns, not significant.

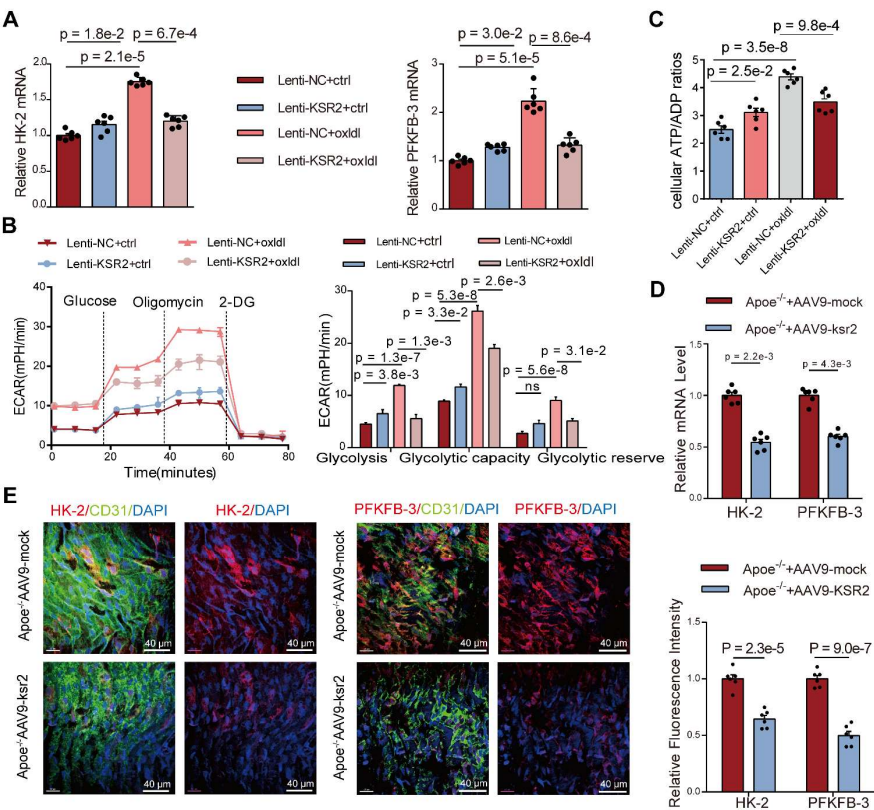


Figure S11

In vivo validation of the effect of endothelial *KSR2* overexpression on AMPK signaling pathway. **A**, Western blot was used to assess the levels of p-AMPK α^{T172} , AMPK $\alpha1$, AMPK $\alpha2$, p-ACC1^{S79}, and ACC1 proteins in the aortic tissue of Apoe^{-/-} + AAV9-mock and Apoe^{-/-} + AAV9-*KSR2* mice. n = 6, statistical analysis of p-AMPK α^{T172} , AMPK $\alpha1$ results were performed using 2-tailed unpaired Mann–Whitney U test due to non-normally distributed data, levels of AMPK $\alpha2$, p-ACC1^{S79}, and ACC1 were analyzed with 2-tailed unpaired Student's t-test. **B**, RT-qPCR was used to investigate the mRNA levels of AMPK $\alpha1$ and AMPK $\alpha2$ in the aortic tissue of Apoe^{-/-} + AAV9-mock and Apoe^{-/-} + AAV9-*KSR2* mice. n = 6, 2-tailed Mann–Whitney U tests (multiple t-test framework, one per gene) with Bonferroni adjustment to control the family-wise error rate. ns, not significant.

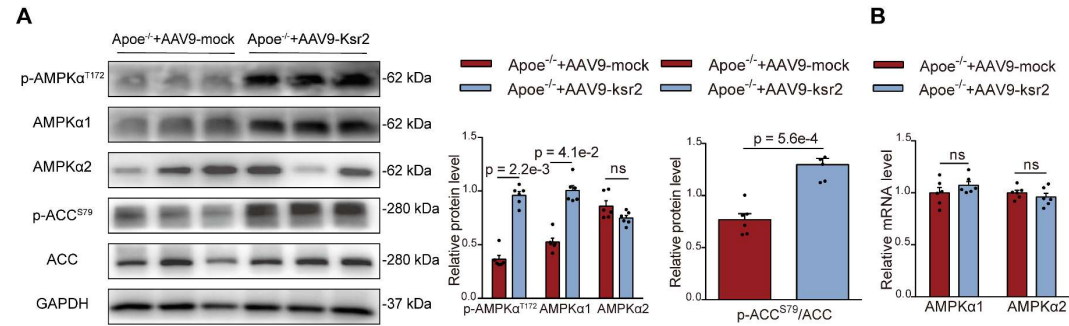


Figure S12

Mechanistic validation of *KSR2*-mediated regulation of *AMPKα1* protein stability. HUVECs were transfected with control siRNA (si-NC) or *KSR2* siRNA (si-*KSR2*) for 48 h, followed by pre-treatment with **(A)** chloroquine (CQ; 10 mM), **(B)** 3-methyladenine (3-MA; 10 mM) and subsequent oxLDL (100 µg/mL) stimulation for 24 h. WB analysis was performed to measure *AMPKα1* protein levels. n = 6, ordinary one-way ANOVA. ns, not significant.

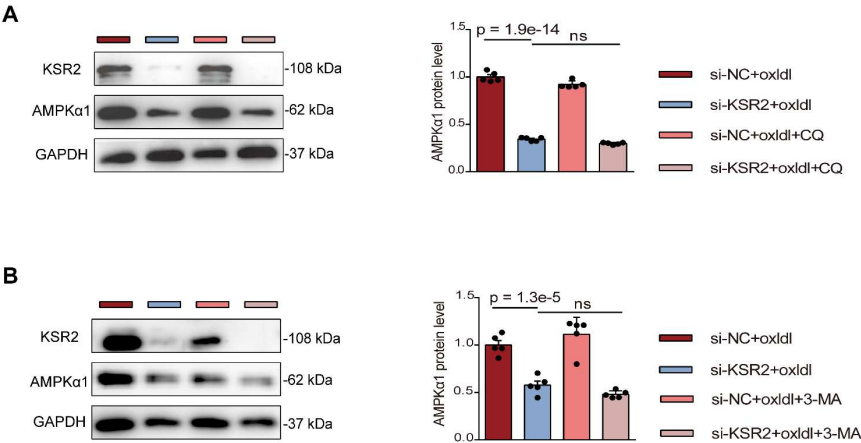


Figure S13

Investigation of the specific ubiquitin chain type mediating *KSR2*-regulated *AMPKα1* ubiquitination in HEK293T cells. HEK293T cells were transfected with *MYC-KSR2*, *FLAG-AMPKα1*, *HA-UB(M0)* (M0-specific mutant), *HA-UB(K6)* (lysine 6-specific mutant), *HA-UB(K11)* (lysine 11-specific mutant), *HA-UB(K27)* (lysine 27-specific mutant), *HA-UB(K29)* (lysine 29-specific mutant), *HA-UB(K33)* (lysine 33-specific mutant) and appropriate control plasmids for 48 h, then treated with MG132 (10 μM) for 24 h. Co-IP and immunoblotting were performed to test the ubiquitination of exogenous *AMPKα1* via immunoprecipitation of *FLAG*-tagged *AMPKα1*.

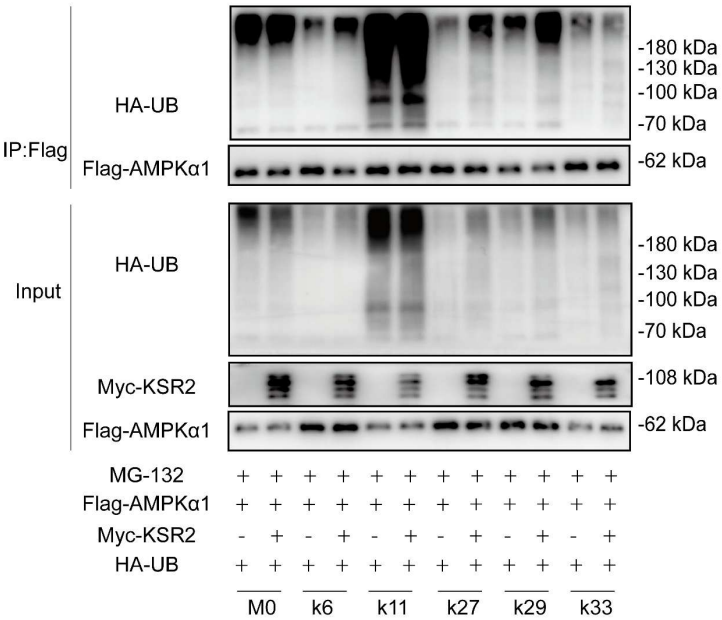


Figure S14

Identification of E3 ubiquitin ligases mediating KSR2-stabilized AMPK α 1 protein. HUVECs were transfected with siRNAs targeting (A) *MKRN1*, (B) *RMND5A*, (C) *TRIM28*, (D) PEDF, (E) Fbxo48, or (F) RNF44, or pretreated with (G) TD165 (0.5 μ M) or (H) lenalidomide (1 μ M), in combination with *KSR2* siRNA for 48 hours, followed by oxLDL stimulation (100 μ g/mL) for 24 hours. AMPK α 1 protein levels were assessed by Western blotting. A–F: n = 5, Kruskal–Wallis test with Dunn’s multiple comparisons test due to small sample sizes. G and H: n = 6, ordinary one-way ANOVA. ns, not significant.

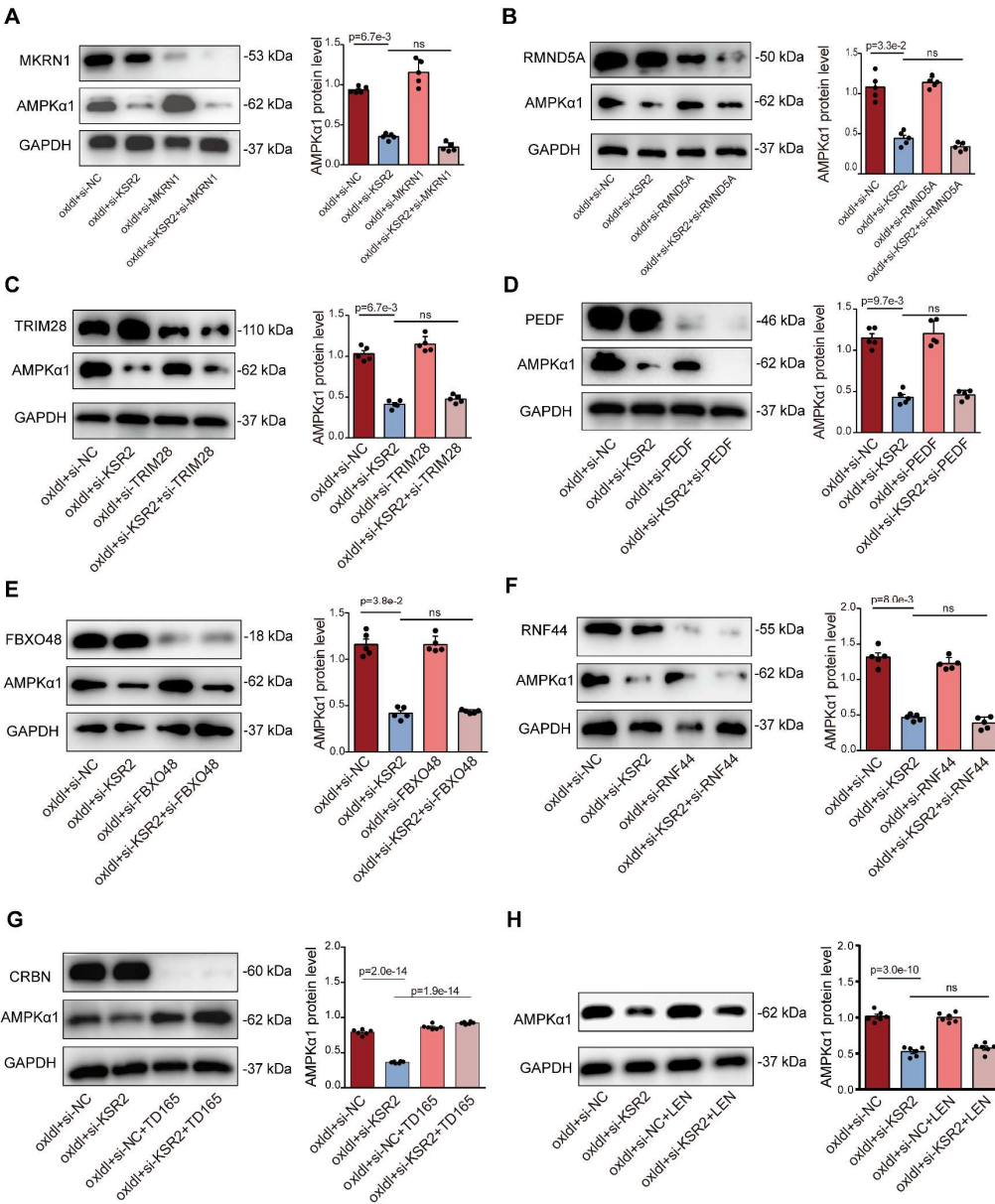


Figure S15

Subcellular localization of *CUL4A*, *DDB1*, and *CRBN* in endothelial cells following oxLDL stimulation. **A** and **B**, HUVECs were treated with oxLDL (100 µg/mL) or vehicle for 24 h. **(A)** Total, nuclear, and cytoplasmic proteins were extracted, and WB was used to analyze the subcellular distribution of *CUL4A*, *DDB1*, and *CRBN*. **(B)** Immunofluorescence co-localization analysis was performed to examine the cellular localization of *CUL4A*, *DDB1*, and *CRBN*. Scale bars = 40 µm.

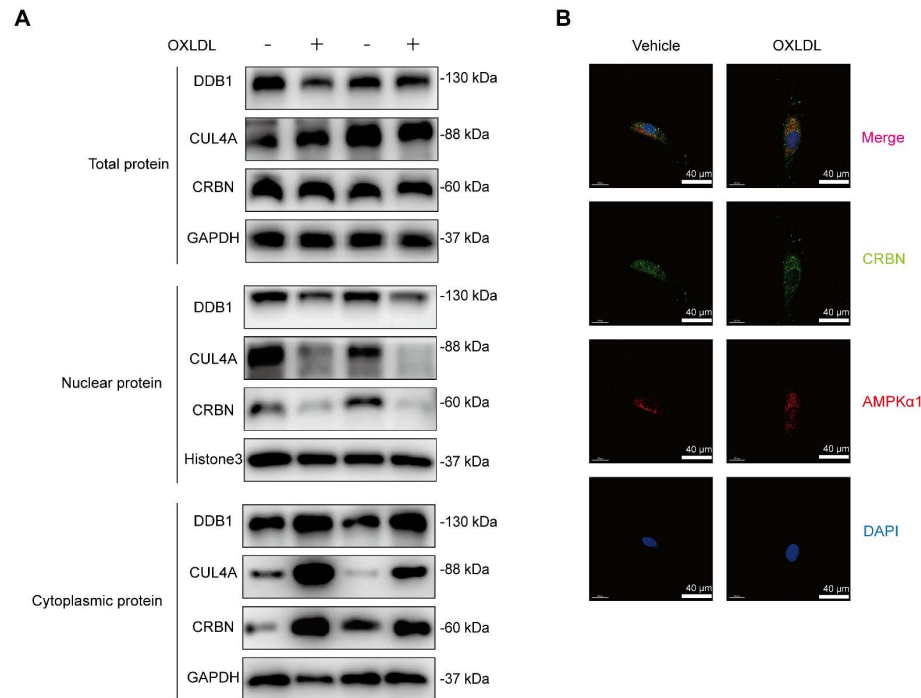


Figure S16

Specific knockdown of endothelial *CRBN* in mice via AAV9-sh*CRBN*. Frozen sections of mouse aortic roots were subjected to double immunofluorescence staining for *CRBN* and the endothelial marker *CD31*, smooth muscle cell marker α -SMA, or macrophage marker *MOMA-2*. Mean fluorescence intensity (MFI) was used to quantify the protein level of *CRBN* in plaque cells. n = 6, 2-tailed unpaired Student's t-test. ns, not significant.

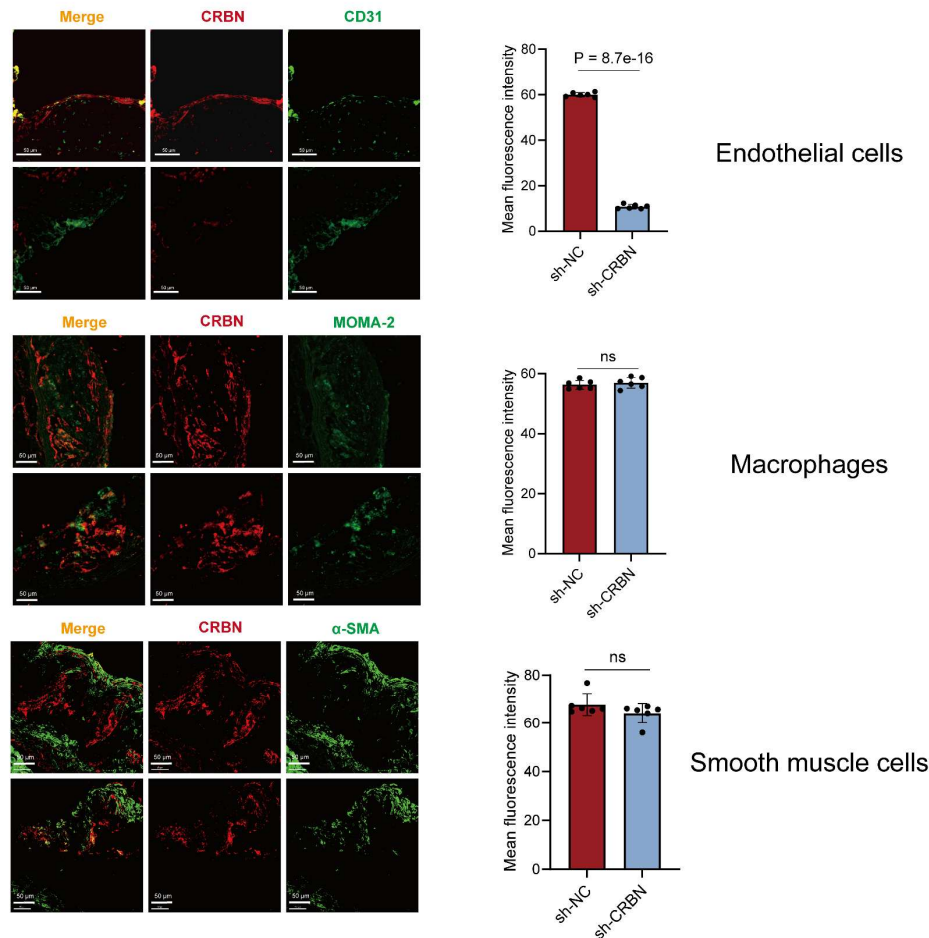


Figure S17

Endothelial *CRBN* knockout suppresses endothelial inflammation and apoptosis, and mitigates atherosclerosis in *ApoE*^{-/-} mice. Endothelial-specific *CRBN* knockout was achieved via tail vein injection of AAV9-ICAM2-sh*CRBN*, while control mice received an equivalent dose of AAV9-ICAM2-shNC. All groups were subsequently pair-fed a high-fat diet for 8 weeks. **A**, Representative en face Oil Red O staining of aortas from *ApoE*^{-/-} + sh-NC and *ApoE*^{-/-} + sh-*CRBN* mice. Quantification of aortic lesion areas is shown. Scale bar = 5 mm. n = 8. 2-tailed unpaired Student's t-test. **B-F**, Representative Oil Red O staining (**B**), H&E staining (**C**), immunohistochemical staining for *MOMA-2* (**D**) and α -*SMA* (**E**), and Masson's trichrome staining (**F**) of aortic root sections from *ApoE*^{-/-} + sh-NC and *ApoE*^{-/-} + sh-*CRBN* mice. Quantification of aortic lesion areas is shown. Scale bar = 400 μ m. n = 8. Statistical analysis was performed using 2-tailed unpaired Student's t-test, except for *MOMA-2* staining results, which were analyzed using the 2-tailed unpaired Mann-Whitney U test due to non-normal distribution. **G**, Immunohistochemical staining of VCAM-1, *TNF- α* in the aortic roots of *ApoE*^{-/-} + sh-NC, *ApoE*^{-/-} + sh-*CRBN* mice. Scale bar = 200 μ m. n = 8, 2-tailed unpaired Student's t-test. **H**, RT-qPCR analysis of VCAM-1 and *TNF- α* mRNA expression in aortas from *ApoE*^{-/-} + sh-NC, *ApoE*^{-/-} + sh-*CRBN* mice. n = 6, 2-tailed unpaired Student's t-test. **I**, Representative en face TUNEL staining of aortic endothelium from *ApoE*^{-/-} + sh-NC, *ApoE*^{-/-} + sh-*CRBN* mice. TUNEL-positive cells are shown in red, *CD31* in green, and nuclei (DAPI) in blue. Scale bar = 20 μ m. n = 6, 2-tailed unpaired Student's t-test. **J**, Western blot analysis of *AMPK α 1*, cleaved caspase-3, Bcl-2, and *Bax* protein levels in aortic tissues from *ApoE*^{-/-} + sh-NC, *ApoE*^{-/-} + sh-*CRBN* mice. n = 6, statistical analysis was performed using 2-tailed unpaired Student's t-test, except for *Bax*/Bcl-2 ratio, which was analyzed using the 2-tailed unpaired Mann-Whitney U test due to non-normal distribution.

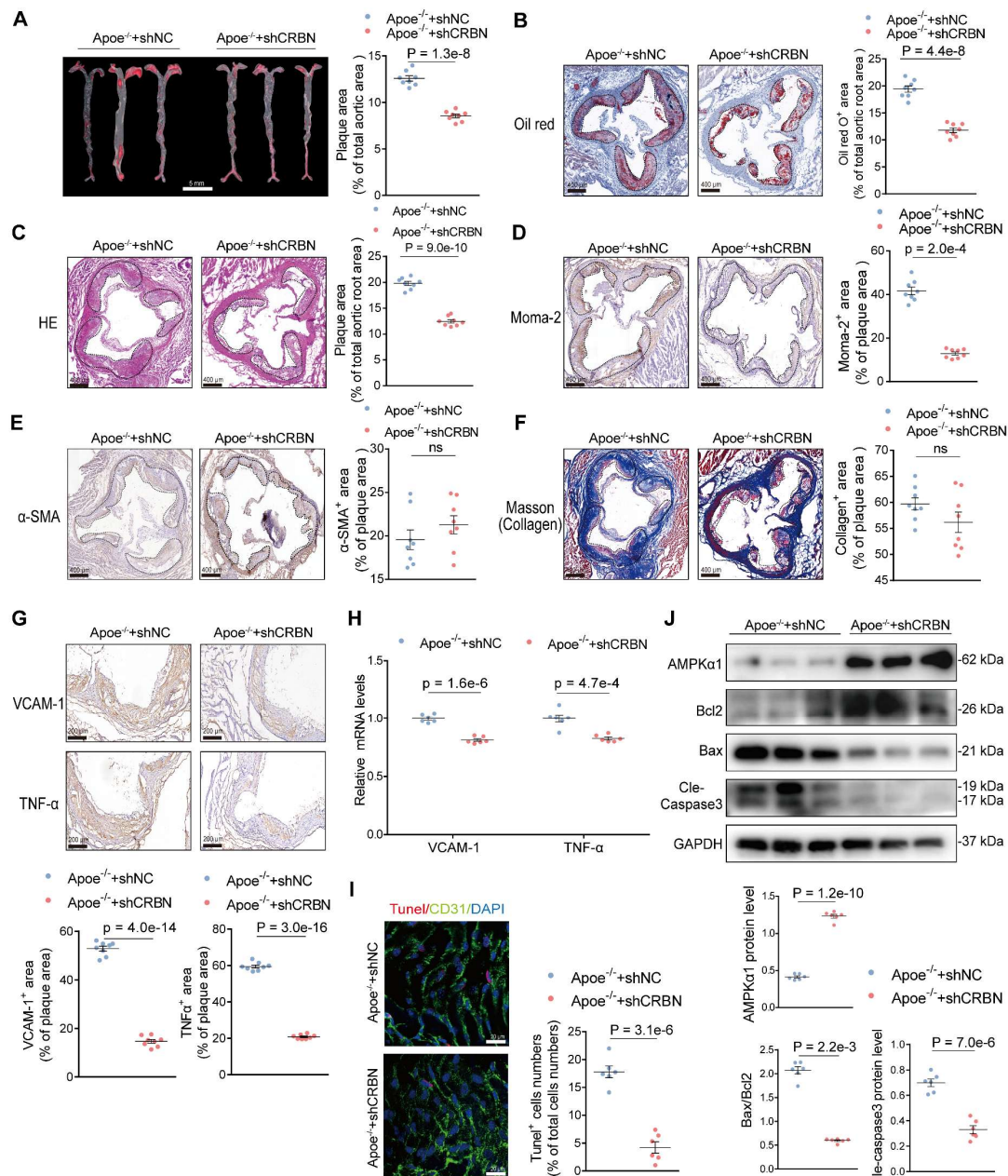


Figure S18

Endothelial *KSR2* Attenuates Atherosclerosis Progression via *CRBN* in *ApoE*^{-/-} Mice. **A**, Representative en face Oil Red O-stained aortas from ApoE^{-/-} + AAV9-mock, ApoE^{-/-} + AAV9-KSR2, ApoE^{-/-} + AAV9-KSR2+ AAV9-CRBN mice. Quantification of aortic lesion areas is shown. Scale bar = 5 mm. n = 8, ordinary one-way ANOVA. **B**, Representative Oil Red O and H&E staining of aortic root cryosections from ApoE^{-/-} + AAV9-mock, ApoE^{-/-} + AAV9-KSR2, ApoE^{-/-} + AAV9-KSR2+ AAV9-CRBN mice. Quantification of aortic lesion areas is shown. Scale bar = 400 μm. n = 8, ordinary one-way ANOVA.

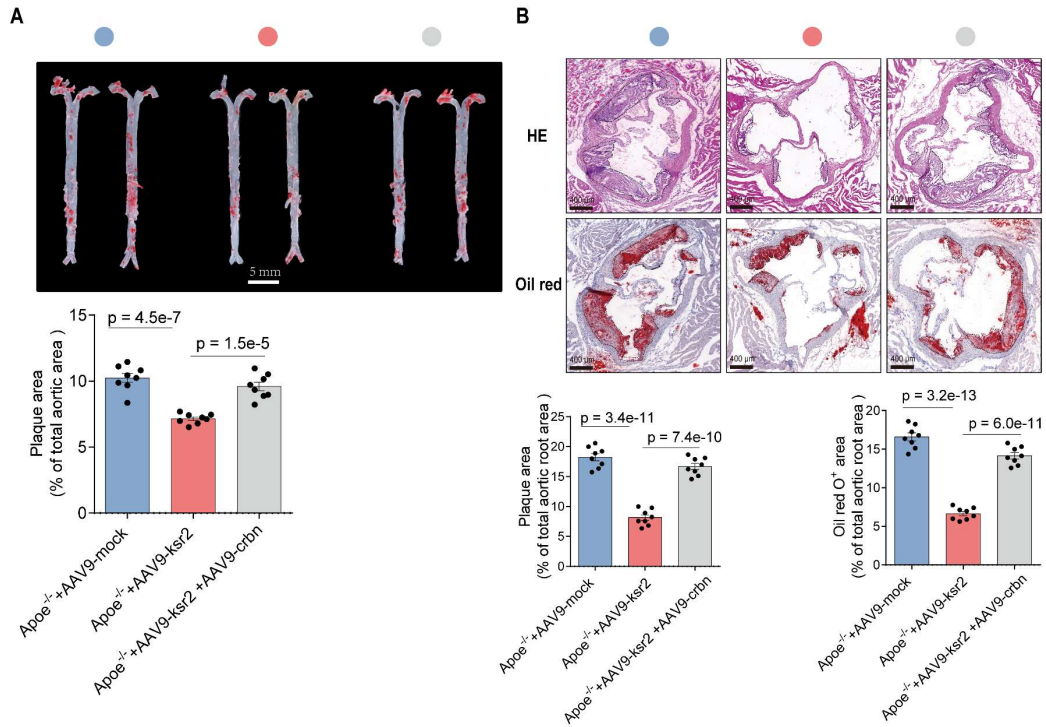


Figure S19

Endothelial *KSR2* maintains glycolytic homeostasis via *AMPKα1*. Lentivirus-stably transfected lenti-*KSR2* HUVECs and lenti-NC HUVECs were transfected with si-NC or si-*AMPKα1* (#1 + 2) for 48 h, followed by treatment with or without oxLDL (100 μg/mL) for 24 h. The cellular ATP/ADP ratio was determined to evaluate energy metabolic shifts in HUVECs. n = 6, ordinary one-way ANOVA.

